SUPPLEMENTARY DATA

Synthesis of DNA hairpins

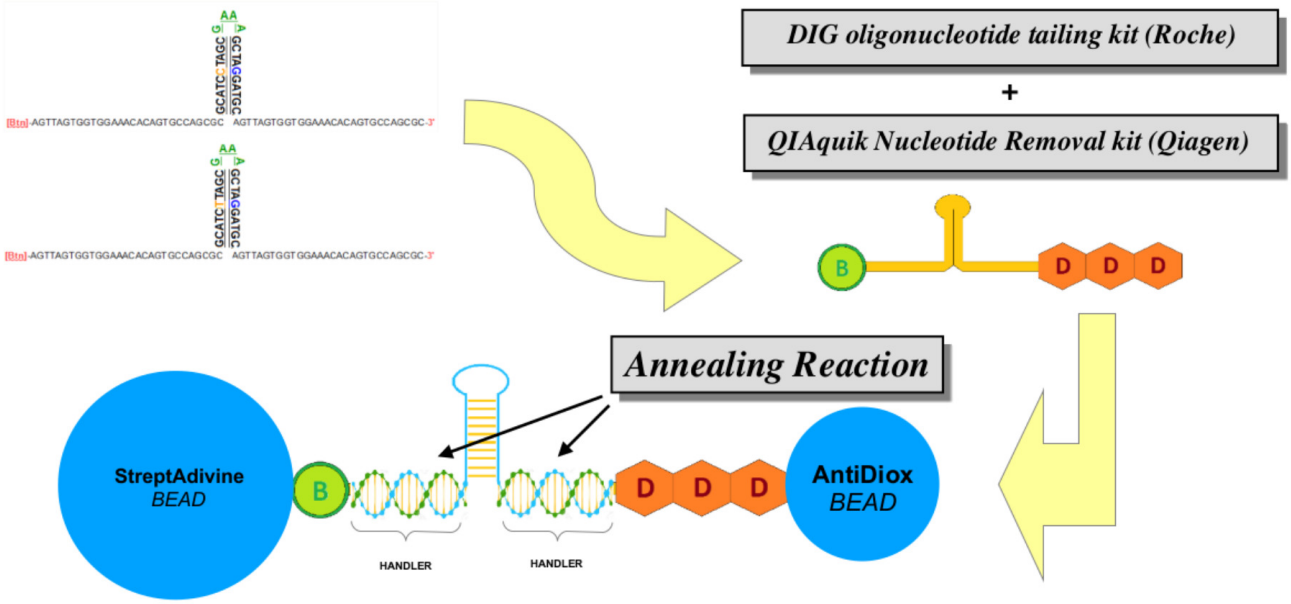

Supplementary Figure 1. Hairpin synthesis. Schematic representation of the procedure used to synthesize the DNA hairpins.

The synthesis of all the hairpins of 10bp and 20bp were performed in 2 general steps, represented in figure 1:

1. Digoxigenin tailing of the 3' end: 1μl of the oligonucleotide (100μM) was tailed using Terminal Transferase from Calf Thymus, recombinant, E. coli (Roche), 1μl (100μM) of dATP (Roche), 1μl (100μM)Digoxigenin-dUTP (Roche), 5μl of 4x $CoCl_2$ solution, 4μl of reaction buffer and 8μl of water (total volume $V_T = 20\mu$l). The product is then purified using the Qiaquick Nucleotide Purification Kit (QIAGEN) and resuspended in 50μl of 10mM Tris pH 7.5 buffer, giving rise to a final concentration of the oligo of 2μM.

2. Annealing reaction: 10pmoles of the DIG-tailed oligo and 20pmoles of the splint were annealed in 50μl of buffer (100mM NaCl and 20mM Tris pH 7.5). The temperature of the dilution is kept 10 min at 70 °C, 10 minutes at 55 °C, followed by decreasing 1 °C every minute until 4 °C is reached.

Oligo	Sequence
10bp	5′-Biotin-AGT TAG TGG TGG AAA CAC AGT GCC AGC GCG CAT C**C**T AGC GAA AAG CTA GGA TGC AGT TAG TGG TGG AAA CAC AGT GCC AGC GC-3′
20bp	5′-Biotin-AGT TAG TGG TGG AAA CAC AGT GCC AGC GCG CGC CGC ATC **C**TA GCA TAT TAG AAA ATA TGC TAG GAT GCG GCG CAG TTA GTG GTG GAA ACA CAG TGC CAG CGC-3′
splint	5′-GCGCTGGCACTGTGTTTCCACCACTAACT-3′

Table 5. DNA oligos used for the DNA hairpins synthesis. The base in black of the 10bp and 20bp oligos are kept for the unmodified hairpin, or changed by an Adenine (for the G-A mismatch) or by a Thymine (for the G-T mismatch).

Obtaining the free energy difference between folded and unfolded states

The free energy difference for the unfolding transition at non-zero force, $\Delta G_{NU}(f)$, is recovered from the zero-force one, ΔG^0_{NU}, by subtracting the reversible work done to orient the molecule along the pulling force axis. The contribution to this work in the force ensemble, due to the optical trap and the handles are equal for both the folded and unfolded state, hence the only free energy contributions are due to the hairpin. Depending on the hairpin state, folded or unfolded, the contributions are:

(i) the orientation of the dsDNA of the hairpin about its main axis (Eq.6)

(ii) the stretching contribution of the released ssDNA upon hairpin unfolding (Eq.7).

Both stretching contributions for hairpin orientation and ssDNA stretching rely on the force-extension relationships. The former is described by a freely-jointed chain (FJC) model with the Kuhn length taken equal to the hairpin diameter, $d = 2.0$nm:

$$x_{orient}(f) = d\left[\coth\left(\frac{fd}{k_BT}\right) - \frac{k_BT}{fd}\right]. \tag{6}$$

The latter is obtained by considering the ssDNA fragment of the number of nucleotides of the unfolded hairpin, described by a worm-like-chain (WLC) model, using an interpolation formula[59], with a persistence length $\xi = 1.35$nm and nucleotide unit length of 0.585nm (both parameters values coming from a best fit to the WLC curve for single-strand DNA in short hairpins[30]):

$$f_{WLC}(x) = \frac{k_BT}{\xi}\left[\frac{1}{4(1-x/L_0)^2} - \frac{1}{4} + \frac{x}{L_0}\right]. \tag{7}$$

This equation can be inverted by means of a Legendre transform into $x_{ssDNA}(f)$. The final expression for the non-zero force of the free energy of the folding-unfolding transition is then:

$$\Delta G_{NU}(f) = \Delta G^0_{NU} - \int_0^f x_{ssDNA}(f')df' + \int_0^f x_{orient}(f')df', \tag{8}$$

where ΔG^0_{NU} is obtained using the kinetic rate theory, described in the main text.

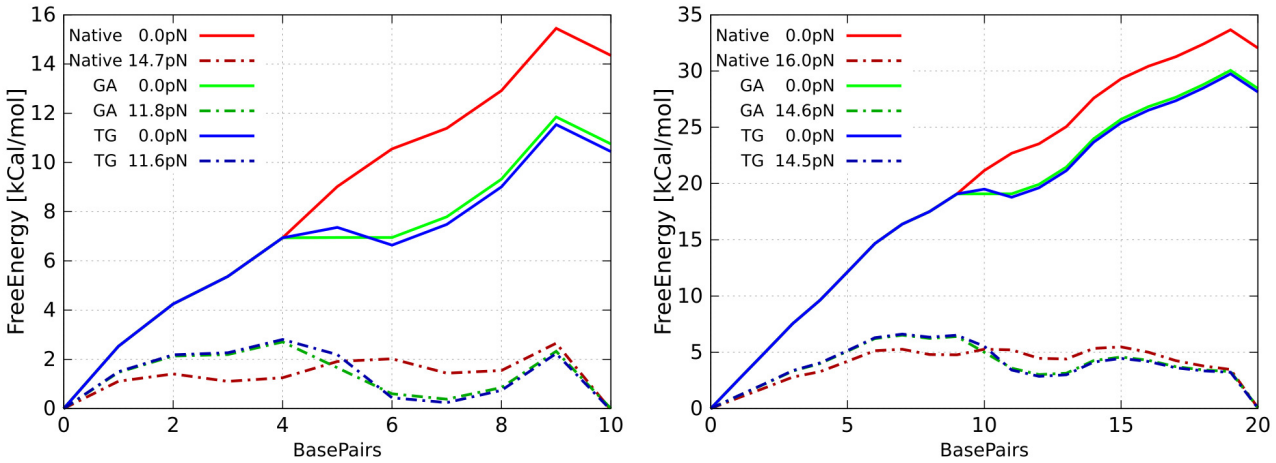

Supplementary Figure 2. Free Energy Landscape of the 10bp (left) and 20bp (right) DNA hairpin. Different color represent the native (red), GA mismatches (green) and GT mismatch (blue) sequence. The continuous line represent the free energy landscape obtained with the NN model at zero force considering the contribution of the tetraloop as obtained from the mfold Web Server. The dashes line represent the FEL at the coexistence force. The contribution of the unfolded bases is estimate using the WLC model for different contour length and subtracting (when at least one bp is still folded) the orientation of the dsDNA. Due to the different ΔG_{NU} the coexistence force is different for the native sequence and the mismatched sequences, this is also reflected in a different extension between the folded and unfolded state (see Tables 1-2)

Hidden Markov Model

In the hopping experiments analysis we extract information on the hairpin states and transition kinetics using the Hidden Markov Model (HMM)[60]. The hidden Markov model is a probabilistic method for the study of time series. It quantifies the likelihood of a model to interpret a series of data and using the iterative Baum-Welch algorithm it is possible to fit the parameters of the model and maximize the likelihood.

The initial parameters of the model are the number of hidden states, the initial probability $\{w_n^0\}$ associated with each state and the transition matrix T_{nm}. The matrix describes the probability that a state m after one step jumps to state n and it is taken as time homogeneous. The transition rate between states could then be read from the off-diagonal elements of the matrix (eventually dividing by the time-step if we want to switch from discrete to continuous time). Given the finite series of force observations $F = (f_1, f_2, f_3, ..., f_T)$ taken from the instrument at a fixed sampling rate, we start from the tentative hypothesis that the system can occupy two states with Gaussian distributed forces (Suppl.Fig.3-5). This introduces two additional parameters in the algorithm for each hidden state: the mean $\bar{f}_n$ and standard deviation $\bar{\sigma}_n$. By means of successive iterations, the maximum likelihood of the model can be computed, and the parameters describing the series F can be optimized.

The two-state model is validated *a posteriori* by looking at the experimental force distributions (e.g. in Fig.2a and Suppl.Fig.3-5) and comparing the likelihood of the two states model ($N = 2$) with a model with $N > 2$ states. In fact, no hidden states beyond the two folded/unfolded configurations emerged from this analysis. The optimized parameters give an estimation of the average force in the folded/unfolded state with the associated standard deviation, the kinetic rate coefficients k^+, k^- of the folding/unfolding process, and the probability w_U, w_N of either state in the hopping experiment, at a given trap position λ.

Repeating this analysis for different λ, see Suppl.Fig.3-5, one can extract the force dependence of the kinetic rates.

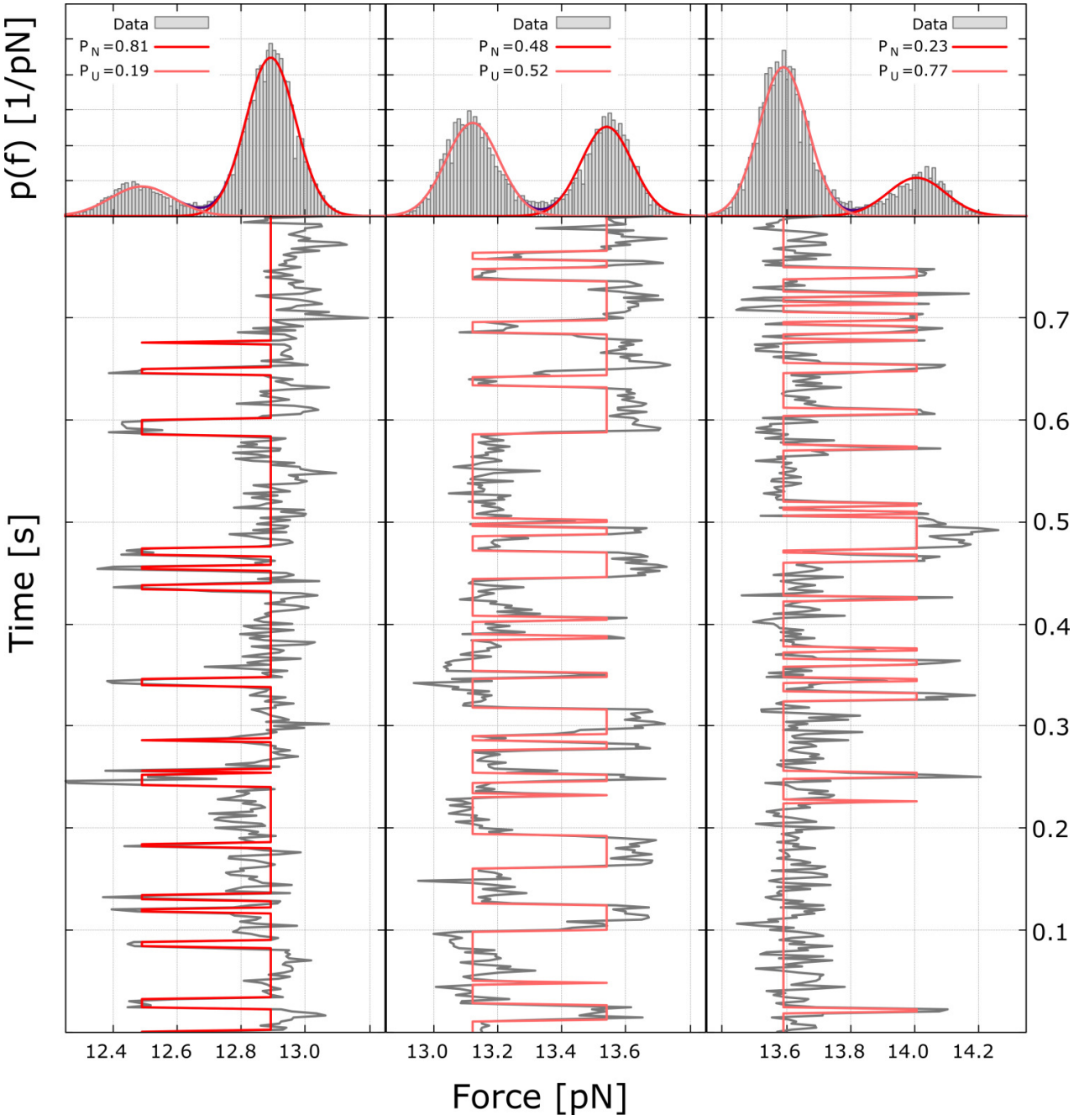

Supplementary Figure 3. Example of HMM analysis in the 10bp native hairpin. Experimental force-time traces (gray) for the 10pb native hairpin during hopping experiments with LOT and the corresponding force histogram (gray bars). In the force time series, hidden by the noise, we observe multiple jumps between the two states as determined by the two force levels evidenced in the force histogram Gaussian peaks (upper panels). These two peaks correspond to the folded (higher force) and the unfolded (lower force) states of the hairpin. The HMM extracts information about the hopping kinetics by determining the optimal trajectory for a given time series (shown in red overlapped to the original grey signal). The two optimized Gaussian force distributions are shown in the upper panels for the P_N folded (bright red) and P_U unfolded (pale red), and compared with the experimental force histograms (grey bars). This analysis is repeated for different values of λ (increasing from left to right). Here is shown $0.8s$ of the whole 15-30s force time series for three conditions close to the coexistence force: $P_N > P_U$ (left); $P_N, P_U \simeq 0.5$ (middle); $P_N < P_U$ (right). The values of P_N, P_U are shown as legends in the upper panels.

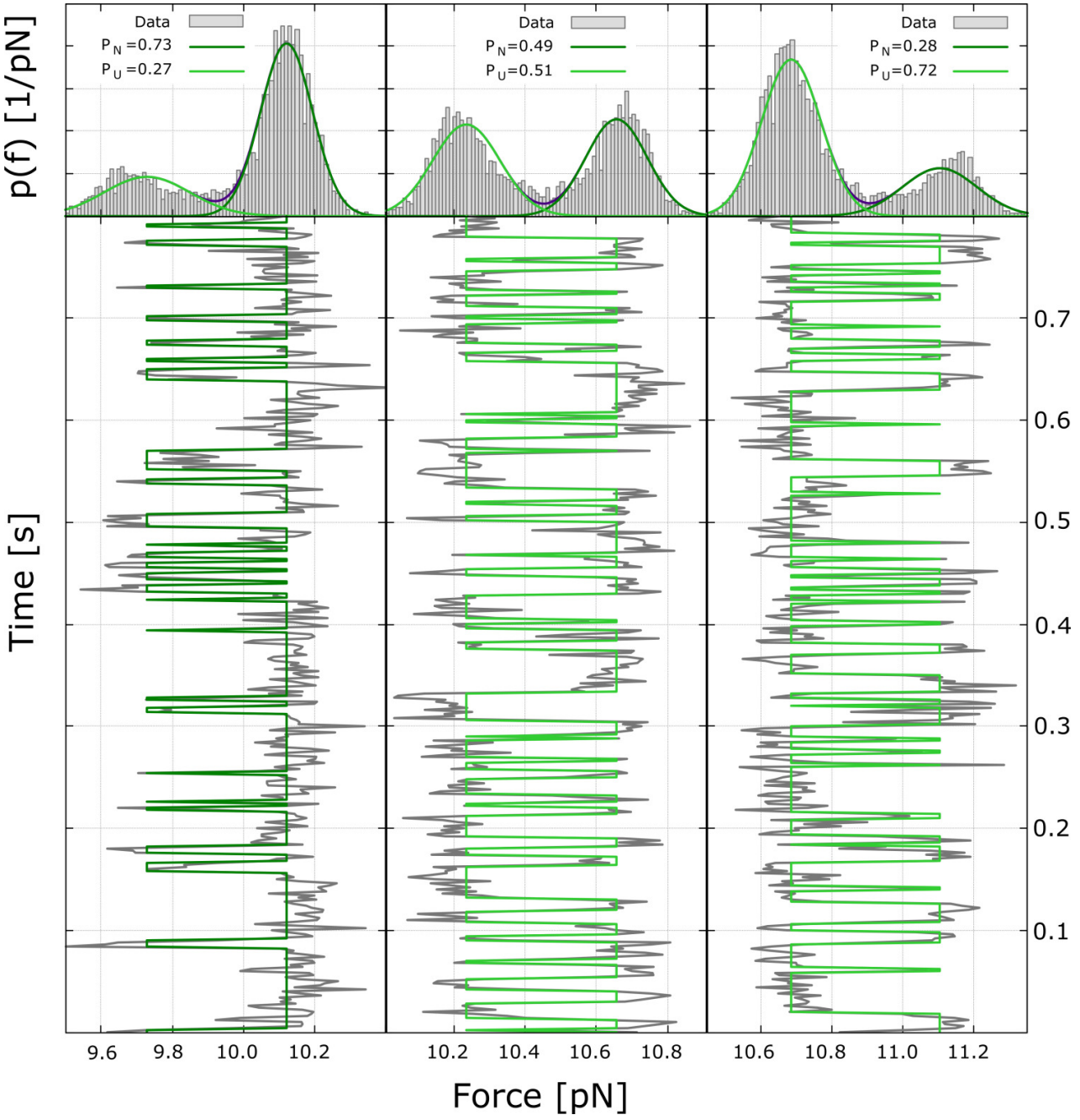

Supplementary Figure 4. Example of HMM analysis in the 10bp hairpin with GA mismatch. Same as in Suppl. Fig.3 for the 10bp hairpin with a GA mismatch, the main difference is in the color of the curves obtained from the HMM that are now green according to the color code used in Fig.2. Comparing these plots with the previous ones in Suppl.Fig.3 we observe that the value of the average hopping force at coexistence (middle panels) changes from $\sim$ 13.4pN in the native sequence to $\sim$ 10.4pN in the mismatch GA sequence.

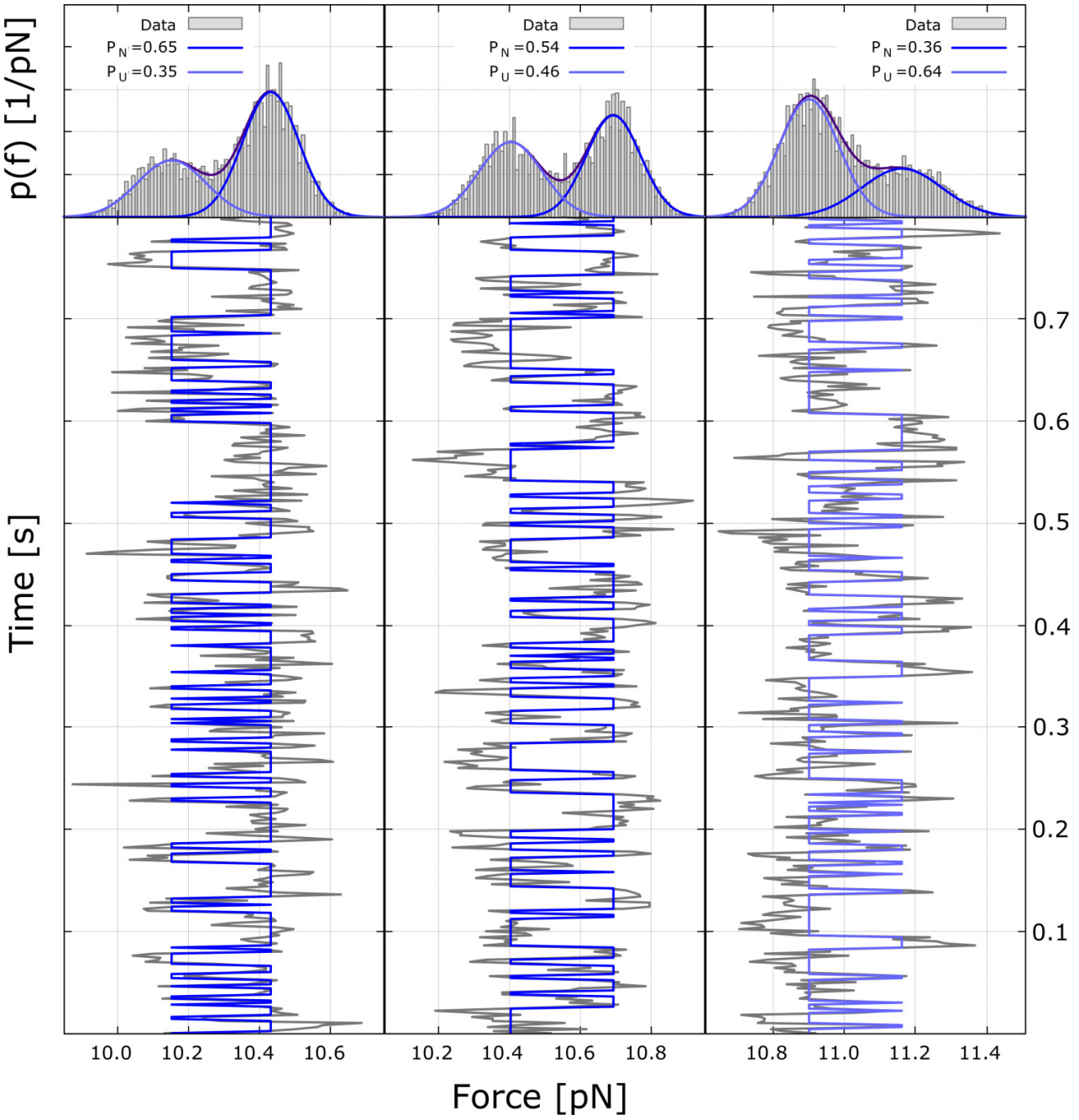

Supplementary Figure 5. Example of HMM analysis in the 10bp hairpin with GT mismatch defect. Same as in Suppl. Fig.3 for the 10bp hairpin with a GT mismatch defect, the color of the curves obtained from the HMM is blue in agreement with the color code used in Fig.2. Comparing these plots with the previous ones in Suppl.Fig.3 we observe that the value of the average hopping force at coexistence (middle panels) changes from $\sim$ 13.4pN in the native sequence to $\sim$ 10.6pN in the mismatch GT sequence. Such a difference cannot be appreciated comparing with the mismatch GA sequence (Suppl.Fig.4).

Pulling experiments 20bp hairpin.

The data analysis of force pulling experiments on the 20bp hairpin is done in four steps:

1. **Drift suppression.** The force pulling trajectories are aligned to eliminate drift effects. Drift effects are small in a single pulling cycle, however they are not along the entire measurement process (typically lasting for 50-100 cycles) as drift tends to accumulate with time leading to net shifts in FDC of a few *nm*. We used an alignment software that substantially compensates for such accumulated drift. Examples of aligned trajectories are plotted in the upper part of Suppl. Fig. 6-8.

2. **Rupture force measurements.** Each unfolding trajectory is checked to identify the value of the force (first-rupture force) at which a force rip is observed for the first time along the unfolding trajectory (red trace in the upper panels of Suppl. Fig. 6-8). Analogously, for each refolding trajectory we identify the value of the force (first-folding force) at which a positive force jump is observed for the first time along the refolding trajectory (blue trace in the upper panels of Suppl. Fig. 6-8).

3. **Rupture force distributions.** First-rupture and first-folding forces are collected among the recorded trajectories to extract rupture-force distributions (central panels in Suppl. Fig. 6-8) for unfolding (red bars) and folding (blue bars).

4. **Kinetic rates.** From the rupture force distributions and using Eq.5 we extract the kinetic rates for the unfolding and refolding process (bottom panels in Suppl. Fig. 6-8). The coexistence force is identified by the value of the force at which the unfolding and folding rates are equal.

The analysis is repeated for different molecules of a given sequence (native, GA, GT) pulled at 100nm/s. Rupture force distributions and kinetic rates are averaged over the molecules, the results are shown in Fig.4 (main text). In figure Suppl. Fig. 6-8 we present results obtained for three different molecules pulled at 100nm/s. Pulling experiments were repeated at different pulling speeds (100,200,300 nm/s, Suppl. Fig.9). While the hysteresis between unfolding and refolding trajectories increases with the pulling speed, the estimated values of the coexistence forces do not vary substantially much, as expected.

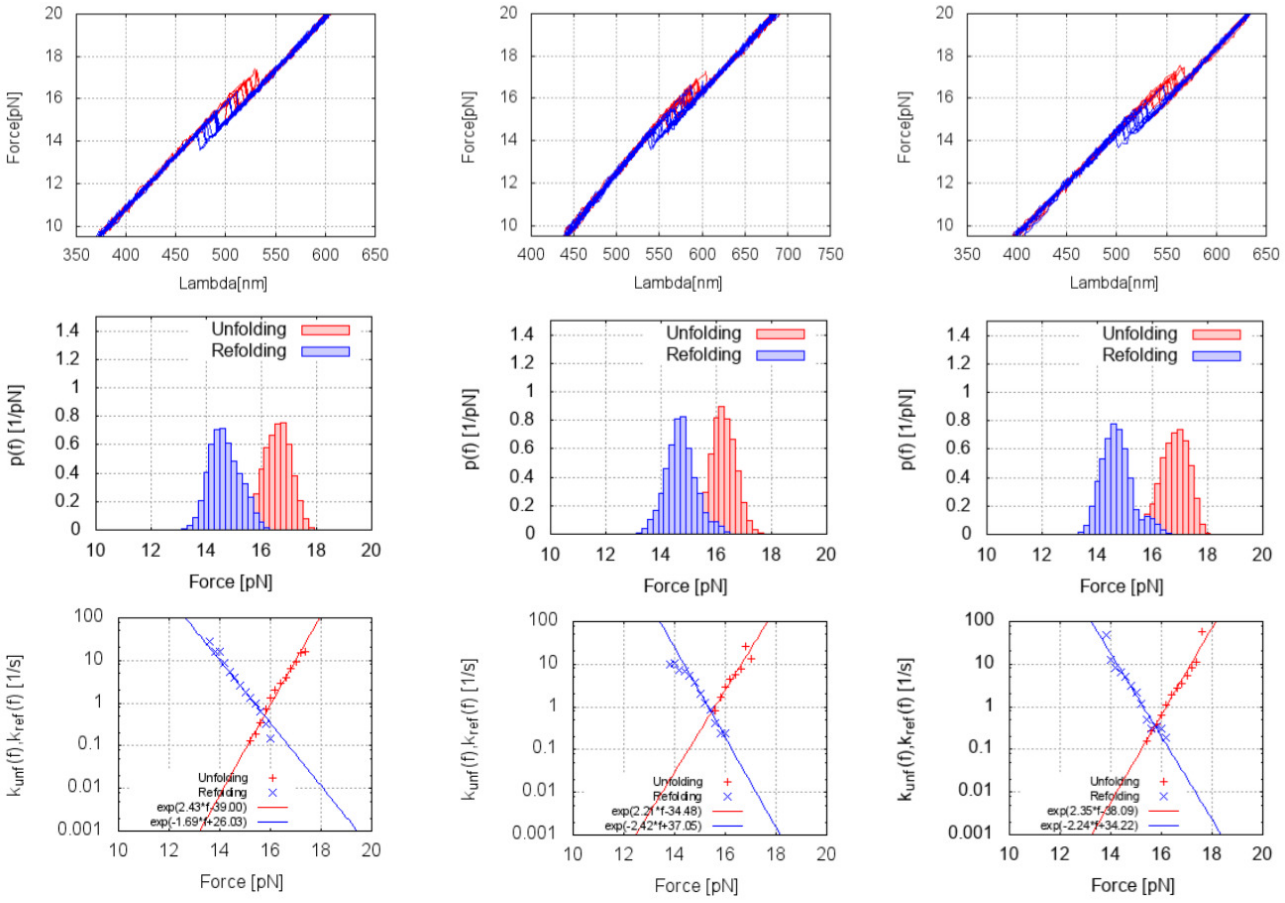

Supplementary Figure 6. Pulling experiments on three molecules of the 20bp hairpin with native hairpin sequence, at pulling speed 100 nm/s. Upper row: FDC (red trajectory for unfolding, blue trajectory for refolding). Middle row: the corresponding rupture force distribution histograms. Bottom row: force-dependent reaction rates $k^{+}(f)$ (unfolding, red) and $k^{-}(f)$ (folding, blue).

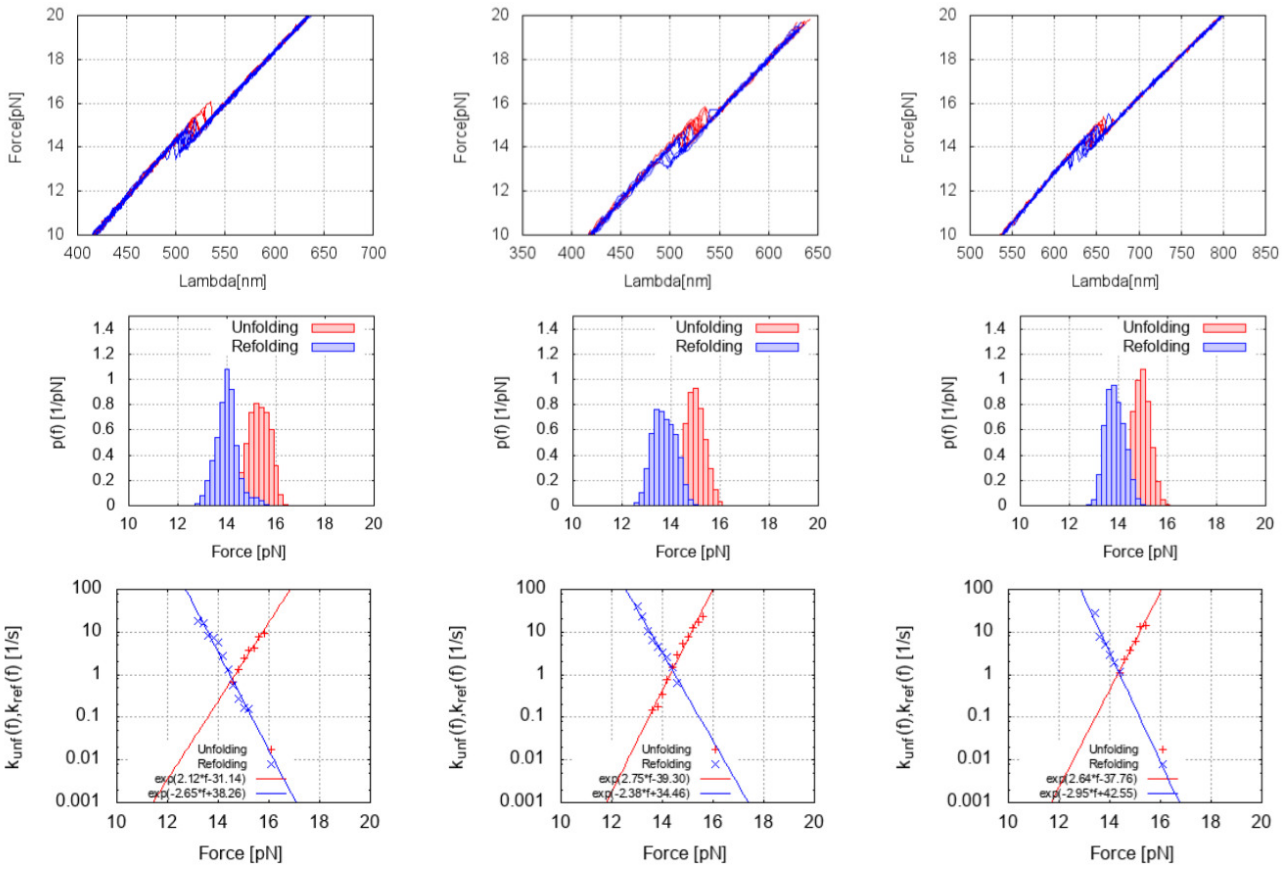

Supplementary Figure 7. Pulling experiments on three molecules of the 20bp hairpin with GA mismatch hairpin sequence, at pulling speed 100 nm/s. Rows and panels are defined as in Suppl. Fig. 6.

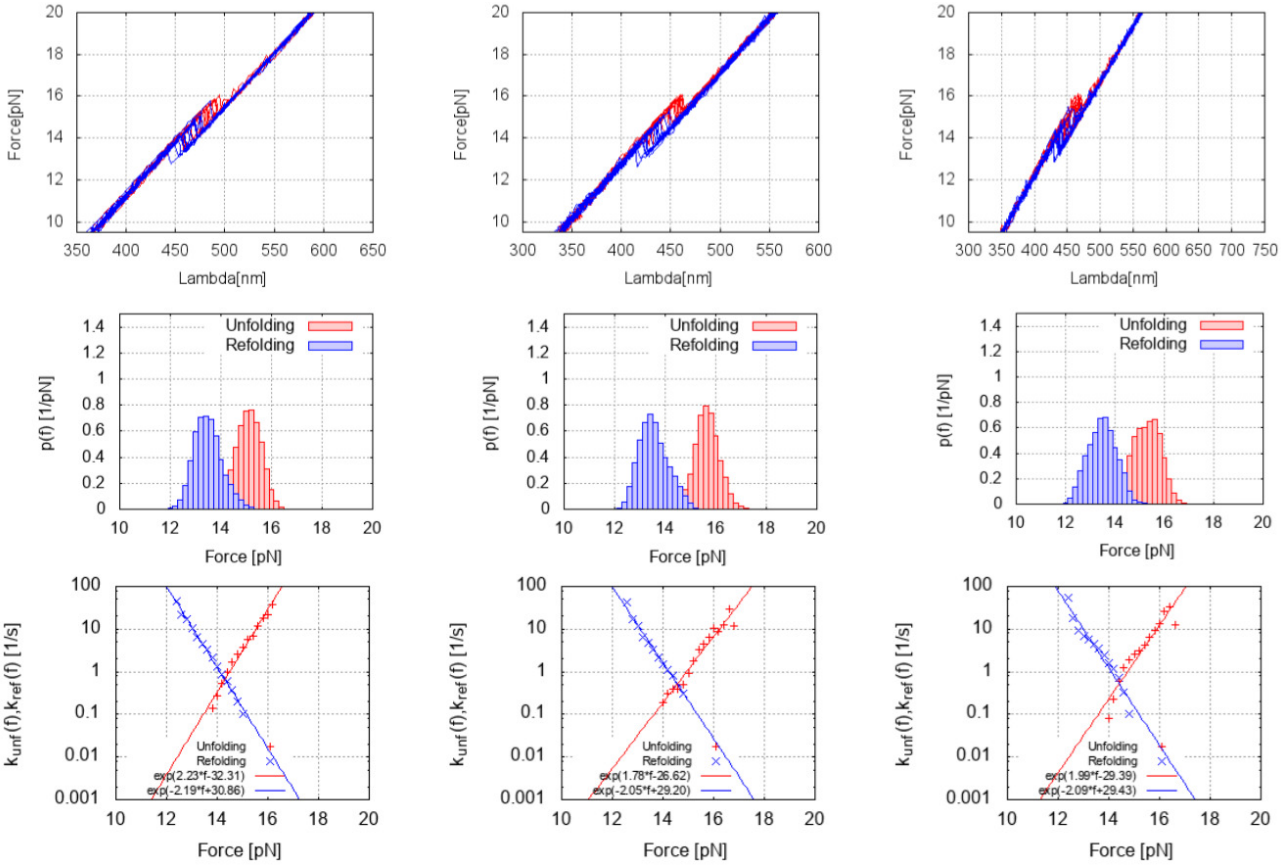

Supplementary Figure 8. Pulling experiments on three molecules of the 20bp hairpin with GT mismatch hairpin sequence, at pulling speed 100 nm/s. Rows and panels are defined as in Suppl. Fig. 6

.

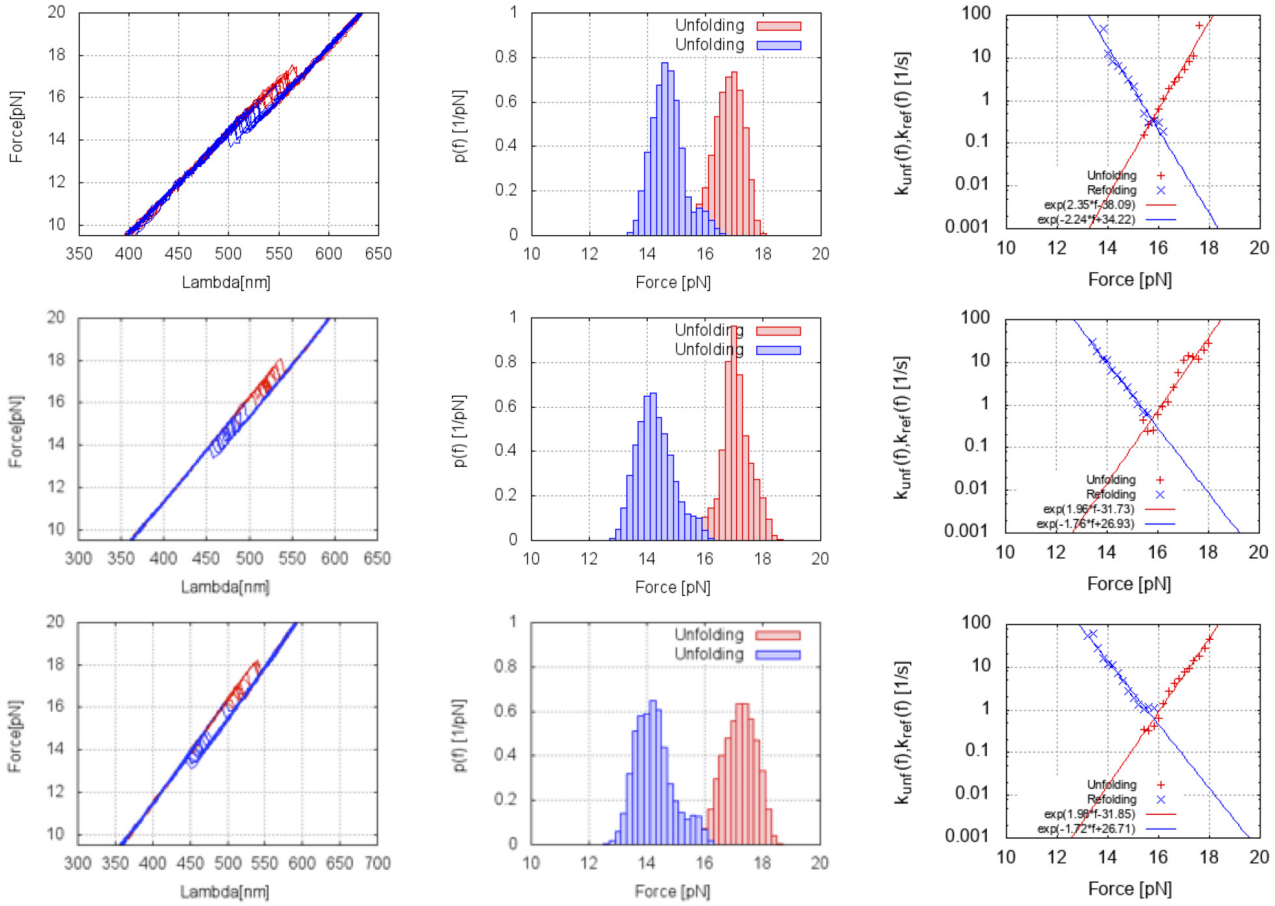

Supplementary Figure 9. Summary of force-pulling experiments for the native 20bp hairpin, at different pulling speeds. From top to bottom, v_{pull} =100, 200, 300 nm/s. Left column: unfolding(red) and refolding (blue) trajectories; each experiment corresponds to about 100 cycles; the rupture force corresponds to the nearly vertical jumps between each pair of trajectories. Central column: histograms of the first-rupture force for unfolding (red) and folding (blue) trajectories; for clarity, the data are convoluted with a Gaussian smearing function with σ =0.2. Right column: unfolding (red) and folding (blue) kinetic rates, $k^+(f), k^-(f)$; crosses are the experimental data, straight lines are exponential fits according to the Bell-Evans model.

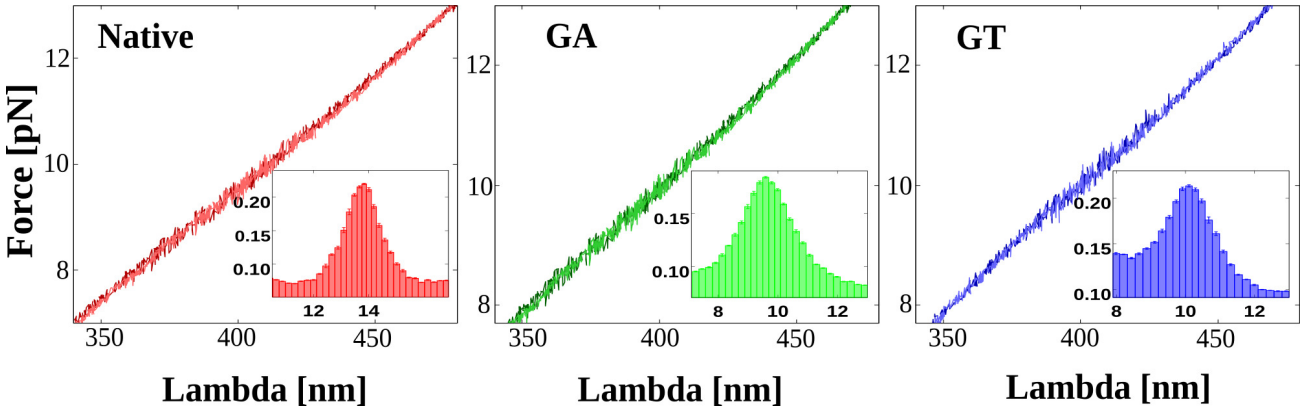

Supplementary Figure 10. 10bp hairpin pulling experiments. Example of a pulling trace of the 10bp hairpin at constant pulling speed 50nm/s for the native hairpin (red), G-A mismatch (green) and G-T (blue). The unfolding trajectory is represented in dark colors and folding trajectory in light colors. Compared to previous pulling experiments for the 20bp, we observe a smaller force rip and faster unfolding and folding kinetic rates (with multiple folding-refolding transitions being observed for each single trajectory). This makes rupture force events noisy and difficult to analyze. In the inset it is possible to observe an increase of the mean square fluctuation of the force close to the coexistence value. This shows the existence of rapid transitions between the folded and the unfolded state even if the noise in the FDC hide the sudden jumps observed in the 20bp hairpin. The coexistence force values obtained in hopping experiments for the 10bp hairpin (main text) are in agreement with the force values at which the mean square fluctuation of force is maximum.